Journal of the Serbian Chemical Society
JSCS@tmf.bg.ac.rs • www.shd.org.rs/JSCS
J. Serb. Chem. Soc. *88* (12) 1265–1278 (2023)
JSCS–5694
Original scientific paper
Published 19 December 2023

Reactions of 2-acetylpyridine-aminoguanidine with Cu(II) under different reaction conditions

MARIJANA S. KOSTIĆ*#, NIKOLA D. RADNOVIĆ#, MARKO V. RODIĆ#, BERTA BARTA HOLLÓ#, LJILJANA S. VOJINOVIĆ-JEŠIĆ# and MIRJANA M. RADANOVIĆ#

University of Novi Sad, Faculty of Sciences, Trg Dositeja Obradovića 3, 21000 Novi Sad, Serbia

(Received 7 July, revised 28 July, accepted 8 September 2023)

Abstract: Aminoguanidine derivatives are the focus of research because of their various biological activities, such as antiviral, antibacterial, analgesic, antioxidant and anticancer. Their complexes with different metals are also examined and many of them show significant biological activity, too. Besides, some of the complexes show good photoluminescent properties and are used for the preparation of photoelectronic devices. Therefore, the synthesis, physicochemical, structural and thermal characterization of the complexes of 2-acetylpyridine-aminoguanidine (L) with copper (II) are described here. Under different reaction conditions, Cu(II) with L gives three complexes of different compositions. By varying the strength of basicity of the deprotonating agent used, it was proven here that the Schiff base given here could be coordinated in neutral or monoanionic form. In the presence of pyridine, a coordination polymer is obtained, while in the presence of ammonia/lithium acetate two different monomeric complexes were crystallised. Their physicochemical and thermal properties, as well as molecular and crystal structure, are determined.

Keywords: Schiff base; Cu complex; synthesis; crystal structure; thermal decomposition; structural characterization.

INTRODUCTION

Aminoguanidine was used as a drug for the treatment of diabetic complications, *i.e.* kidney disease, due to its ability to lower the level of advanced glycation end products.[1] However, some serious side effects were present, thus its Schiff bases were suggested as more suitable for the application.[2,3] Since the chelation, *i.e.*, the metal centre could have a positive effect on the biological activities of Schiff bases,[4] it is not surprising that the metal complexes with these ligands are widely studied.[5,6] Some of them were found to express various bio-

* Corresponding author. E-mail: marijana.kostic@dh.uns.ac.rs
# Serbian Chemical Society member.
https://doi.org/10.2298/JSC230707060K

logical effects, such as antiviral, antibacterial, analgesic, antioxidant, and even anticancer activity.[7] On the other hand, some of the complexes showed high photoluminescence and were used for the preparation of optoelectronic devices.[8]

The examination of the crystal structure of metal complexes with aminoguanidine Schiff bases started with the work of Leovac et al.[9] and since then numerous complexes were synthesised, characterised, and their possible applications investigated.[10–13]

Among the mentioned Schiff bases, 2-acetylpyridine-aminoguanidine (L) stands out, due to its ability to achieve different coordination modes in the complexes. Namely, depending on the synthetic conditions, this Schiff base could be coordinated or have a role of the counterion.[14] Nonetheless, if coordinated it could act as a tridentate ligand if in its neutral form,[13] or the bidentate ligand if in its monoprotonated form.[12] Since the well-known alkaline nature of the aminoguanidine residue, as well as the fact that the guanidinium group is found in proteins and at physiological pH is protonated, it is of interest to examine the conditions for its deprotonation and the influence of the different substituents attached to it.

Hence, in this paper, three new complexes of copper(II), of which one polymeric cationic $\{[Cu(L)(\mu\text{-}Cl)]NO_3\cdot 0.25H_2O\}_n$ (**1**), and two neutral complexes [Cu(L–H)Cl] (**2**) and $[Cu(L)ClNO_3]\cdot H_2O$ (**3**) were synthetized, and their physicochemical and thermal properties, as well as molecular and crystal structure were determined.

EXPERIMENTAL

Reagents

All chemicals used for synthesis and characterization were reagent-grade and used as received from commercial sources, without further purification, except for the ligand 2-acetylpyridine-aminoguanidine dihydrogendichloride, $[H_2L]Cl_2$, which was prepared according to the previously published procedure.[10]

Preparation of the complex $\{[Cu(L)(\mu\text{-}Cl)]NO_3\cdot 0.25H_2O\}_n$ (1)

To the warm solution of 0.25 mmol (0.063 g) $[H_2L]Cl_2$ in 5 mL H_2O, 0.25 mmol (0.06 g) $Cu(NO_3)_2\cdot 3H_2O$ and 0.5 mL pyridine were added. The mixture was slightly heated until dissolution. The resulting green solution was left at room temperature and after 7 days, green single crystals were filtered and washed with H_2O and EtOH. Yield: 0.064 g (70 %). The same complex was obtained in the reaction of the metal salt (0.25 mmol) dissolved in H_2O (3 mL), and the ligand (0.25 mmol) was dissolved in MeOH (5 mL).

Preparation of the complex [Cu(L–H)Cl] (2)

The warm solution of 0.25 mmol (0.06 g) $Cu(NO_3)_2\cdot 3H_2O$ in 3 mL MeOH was added to a warm solution of 0.25 mmol (0.063 g) $[H_2L]Cl_2$ in 5 mL MeOH, in the presence of the few drops of ammonia. The mixture was mildly heated until dissolution. The resulting solution was left at room temperature and after 7 days brown single crystals were filtered and washed with MeOH. Yield: 0.051 g (71 %).

*Preparation of the complex [Cu(L)ClNO$_3$]·H$_2$O (**3**)*

The warm solution of 0.25 mmol (0.06 g) Cu(NO$_3$)$_2$·3H$_2$O in 2 mL H$_2$O was added to the warm solution of 0.25 mmol (0.063 g) [H$_2$L]Cl$_2$ in 5 mL MeOH, in the presence of the lithium acetate (0.5 mmol, 0.05g). The mixture was slightly heated until dissolution. The resulting dark green solution was left at room temperature and after 7 days blue crystals were filtered and washed with MeOH. Yield: 0.056 g (63 %).

Analytical methods

Elemental analyses (C, H, N) of air-dried compounds were carried out by standard micro-methods. Molar conductivity measurements of freshly prepared solutions (c = 1 mmol L^{-1}) were performed on a Jenway 4010 conductivity meter. IR spectra were recorded on a Thermo Nicolet iS20 FTIR spectrophotometer (Thermo Fisher Scientific) with Smart iTR™ ATR sampling accessories, in a range of 4000–400 cm^{-1}. Thermal data were collected using TA Instruments SDT Q600 thermal analyser coupled to Hiden Analytical HPR20/QIC mass spectrometer. The decomposition was followed from room temperature to 700 °C at a 10 °C min^{-1} heating rate in the argon carrier gas (flow rate = 50 cm^3 min^{-1}). Sample holder/reference: alumina crucible/empty alumina crucible. Sample mass 2.5–3 mg. Selected ions between m/z 1 and 93 through the TG–MS measurements were monitored in multiple ion detection mode (MID).

Single crystal X-ray diffraction

Crystallographic and refinement details are listed in Table S-I of the Supplementary material. All data were collected at room temperature. Crystal structures were solved using the iterative dual-space routine within SHELXT[15] and refined with SHELXL[16]. All non-hydrogen atoms were refined anisotropically, while hydrogen atoms were placed in idealized positions and refined using a riding model.

The presence of water molecule in **1** was confirmed by TGA which matches with the occupancy factor of oxygen that was constrained to 0.25. Hydrogen atoms bonded to O4 in **1** could not be located in the residual density map due to low occupancy.

The final structures underwent internal validation using Platon[17] and external validation using the Cambridge Structural Database (CSD)[18] *via* the Mogul[19] knowledge bases accessible through Mercury CSD.[20]

Analytical and spectral data of the synthesized compounds are given in Supplementary material to this paper.

RESULTS AND DISCUSSION

Syntheses and characterization

The Cu(II) complexes **1**–**3** were obtained in the reaction of the warm solutions of the chloride salt of the ligand and copper(II) nitrate, in a mole ratio of 1:1 in the presence of the deprotonating agent (Scheme 1). The latter was pyridine in the case of complex **1**, ammonia for **2** and lithium acetate for **3**, and was used to deprotonate the Schiff base and enable its coordination. Depending on the strength of the base used as a deprotonating agent, three new complexes with two different degrees of deprotonation of the chelating ligand were isolated. Namely, when pyridine and lithium-acetate were used, the ligand was coordinated in its neutral, and, so far, the most common form.[12] On the contrary, when ammonia

was used, the monoanion of the ligand was coordinated. Since ammonia is a stronger base than pyridine and acetate ions, this is not surprising. The synthesis of complex **1** could be also carried out from the mixture of MeOH and H_2O. It is interesting to mention that the compound in which the monoanion of the ligand is coordinated (**2**) was also obtained during syntheses from methanolic solutions of copper (II) nitrate and chloride salt of the ligand, in the presence of Na_2CO_3 and KOH as diprotonation agents (proven by the results of elemental analysis and IR spectra), which was expected considering the strength of their basicity.

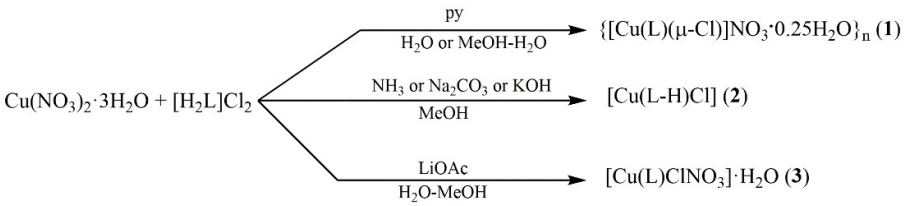

Scheme 1. Synthesis of the complexes.

All three compounds are well soluble in DMF. Complexes **1** and **3** are well soluble in water, as well, while complex **2** is insoluble in this solvent. Methanol dissolves complex **1** well, and the other two complexes moderately, and all three compounds dissolve poorly in ethanol. The molar conductivity values indicate that complex **1** is a 1:1 type electrolyte, thus the polymeric structure is lost. The value of molar conductivity of complex **3** is between 1:1 and 2:1 type electrolytes, which indicates the partial substitution of anionic ligands with solvent molecules. The molar conductivity measurements confirm the non-electrolytic nature of complex **2**.

The ligand coordinates as NNN-tridentate, *via* pyridine, azomethine and the imine nitrogen atom of the aminoguanidine residue, which is primarily assumed by the comparison of IR spectra of the complexes with the spectrum of the ligand. Due to the coordination, ν(CN) band originating from the azomethine group (found at 1684 cm^{-1} in the ligand spectrum) suffers a negative shift of *ca*. 35–40 cm^{-1}. Similarly, the band ascribed to the imine group of the aminoguanidine fragment was shifted from 1624 cm^{-1} (in the ligand spectrum) to 1595–1603 cm^{-1} (in the spectra of the complexes). A band of weak intensity that can be observed in the spectra of complexes, at 647 (**1**), 640 (**2**) and 645 cm^{-1} (**3**), may be assigned as the vibrations of the pyridine ring and confirm its coordination through the nitrogen atom.[10] Also, in the spectrum of **1**, another significant band at 1385 cm^{-1}, recognizable by its very strong intensity, originates from the uncoordinated NO_3^-. On the contrary, in complex **3**, the band occurring at 1299 cm^{-1} originates from the monodentate coordinated nitrate.[21]

Crystal structure description

The molecular structures of all three complexes are presented in Fig. 1, while the selected structural data are summarized in Table I. In all three structures the usual, tridentate coordination mode of the Schiff base, *i.e.*, through pyridine N5, azomethine N3 and imine N1 nitrogen atom of the aminoguanidine residue was found. This coordination mode resulted in the formation of two five--membered chelate rings, one of 2-acetylpyridine and one of aminoguanidine moiety (Fig. 1). In compounds **1** and **3** the ligand is present in its neutral form, and in compound **2** the ligand is present in its monodeprotonated form (deprotonation of the chelate ligand occurs on the hydrazine nitrogen atom N2).

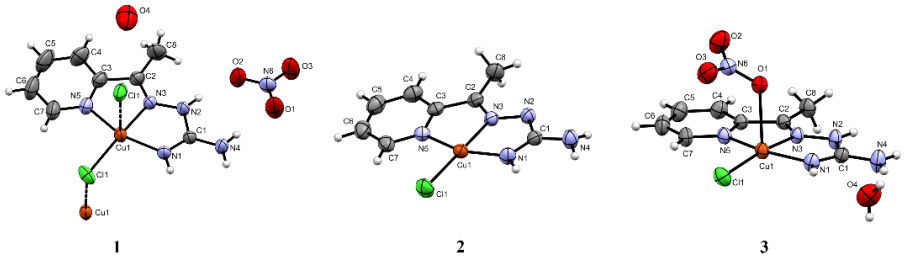

Fig. 1. Molecular structures of complexes **1**–**3**.

In complex **1**, copper (II) is situated in the square-pyramidal environment of the NNN-coordinated chelate ligand, and one chlorido bridge in the basal plane, and another chlorido bridge in the apical position. Deviation from the ideal square-pyramidal geometry, *i.e.*, the deformation towards trigonal-bypiramide, can be described by τ_5 parameter,[22] which for this compound has a value of 0.22 (the square-pyramidal environment of the copper(II) is moderately deformed). The copper (II) ion is shifted from the equatorial plane towards the apical ligand by 0.1159(9) Å. Of the two chlorido ligands, the equatorial one, forms the shorter bond with copper (II), while the apical one is much further away (by even more than 0.6 Å). It is important to mention that complex **1** is the first coordination polymer with this ligand. The monomer units are bridged by chlorido ligands and the Cu···Cu atom separation is 3.742(2) Å. The angle that the copper(II) atom from one subunit subtends with the copper(II) atom from another unit *via* the chlorido ion as a bridge between these subunits (Cl1–Cu1–Cl1^i, Table I) has the value of 97.28(3)°.

In complex **2**, the ligand is coordinated as a monoanion. Copper(II) is placed in the square-planar environment of three nitrogen donor atoms of the ligand and one chlorido ligand. Deviation of this geometry towards tetrahedral is described by τ_4 parameter,[23] which for complex **2** equals 0.16. As in structure **1**, the coor-

dination of Schiff base resulted in the formation of two five-membered chelate rings.

TABLE I. Selected bond lengths and bond angles; Symmetry operation: (*i*) *x*, −*y*+3/2, *z*+1/2

Bond	**1**	**2**	**3**
	Bond length, Å		
Cu1–N1	1.9340(19)	1.9130(17)	1.9393(12)
Cu1–N3	1.9713(19)	1.9523(14)	1.9665(11)
Cu1–N5	2.015(2)	2.0092(16)	2.0177(12)
Cu1–Cl1	2.2372(7)	2.2227(5)	2.2165(4)
Cu1–Cl1^{i}	2.8525(7)	-	-
Cu1–O1	-	-	2.4604(12)
N1–C1	1.298(3)	1.317(2)	1.2954(19)
N4–C1	1.322(3)	1.348(2)	1.3315(19)
N2–C1	1.375(3)	1.364(2)	1.3757(19)
N2–N3	1.352(3)	1.356(2)	1.3573(16)
C2–N3	1.279(3)	1.293(2)	1.2808(17)
Bonds		Bond angle, °	
Cl1–Cu1–N3	172.33(6)	178.64(5)	171.20(4)
N1–Cu1–N5	158.25(9)	159.80(6)	158.37(5)
N1–Cu1–N3	79.87(8)	79.47(6)	79.83(5)
N3–Cu1–N5	78.73(8)	80.34(6)	78.78(5)
N3–Cu1–O1	–	–	92.17(4)
N3–N2–C1	113.31(18)	107.77(14)	113.32(11)
N1–C1–N4	126.6(2)	123.33(17)	126.46(14)
N2–C1–N1	117.1(2)	121.41(17)	117.14(12)
C3–N5–C7	119.2(2)	119.05(17)	119.16(13)

The square-pyramidal copper (II) environment with a τ_5 parameter of 0.21 is found in complex **3**. The basal plane of this pyramid consists of the donor atoms of the chelate ligand and the chlorido ligand, while the apex of the pyramid is occupied by the oxygen atom O2 from the nitrato ligand. Copper (II) is shifted towards the apical oxygen by 0.1221(6) Å. Expectedly, of the three nitrate oxygen atoms, the coordinating one, O1, is at the greatest distance from nitrogen N6 (1.2642(17) Å), while the remaining two, O2 and O3 are at distances shorter by ca. 0.04 and 0.02 Å, respectively. In the polymeric complex **1**, nitrate has a role of a counterion, and the distance of its oxygen atoms from N6 is in the range of 1.221(3)–1.245(3) Å.

The entire ligand system in all three complexes shows a high level of planarity, which is evidenced by the values of the dihedral angles at which the pyridine ring is subtended with the 2-acetylpyridine and aminoguanidine metallocycles (5.9(13) and 3.5(15)° for **1**, 3.82(5) and 1.85(4)° for **2**, and 1.01(10) and 2.78(3)° for **3**, respectively).

In all these complexes, the distances between the Cu atom and chelating ligand donor atoms are in the range 1.9130(17) – 2.0177(12) Å, with Cu–pyridine nitrogen atom bond lengths being the longest, and those with the imine nitrogen atom being the shortest, making the nitrogen N1 a better electron donor than nitrogen N3. In the square-pyramidal structures of **1** and **3**, Cu-coligand bond lengths have also the expected values, with the equatorial ligand are closer to the metal centre and the apical ligand is further from it. In these two complexes, the length of the C1–N1 bond corresponds to the value of the localised double bond, and after coordination, this bond is shortened, compared to its length in the free ligand. The exceptions in the change of some geometric parameters after coordination in **2** and in the other two compounds can be explained by the coordination of the ligand in its monoanionic form (**2**), while in the other complexes, it is coordinated in its neutral form (**1** and **3**).

In **2**, deprotonation of the aminoguanidine residue leads to elongation of the C1–N2 and C1–N4, and shortening of N2–N3 bonds, but this trend is also observed in the structures of the other two complexes, which indicates that the formation of coordination covalent bond has a greater impact on bond lengths than deprotonation. Also, the ligand coordination leads to angular changes in aminoguanidine moiety, visualized through the shrinking of the N3–N2–C1 and N2––C1–N1 angles and widening of the N1–C1–N4 angle in these two complex compounds. The angle N1–C1–N4 has a larger value after coordination in **1** and **3**, but the smallest value in **2**, while the angles N3–N2–C1 and N2–C1–N1 have the same value as before deprotonation.

Besides the electrostatic interactions, the crystal structure of **1** is additionally stabilised by the intermolecular hydrogen bonds (Fig. S-1 of the Supplementary material), which engage all N–H donors of the cation and all three nitrate oxygens as acceptors (Table II). This way of hydrogen bonding affects forming of the layer in the crystallographic *bc* plane, where the nitrate ion connects two chains of monoperiodic cations through the previously mentioned hydrogen bonds (Fig. S-2 of the Supplementary material).

The crystal structures of **2** and **3** are also stabilised by hydrogen bonding. The intermolecular hydrogen bonds were observed in **2** which engages the N4 atom as a donor of two hydrogen bonds and N2 and Cl1 as acceptors. This way of bonding leads to the formation of a chain that extends along the crystallographic [01 $\bar{1}$] direction (Fig. S-3 of the Supplementary material). Crystal water molecules in **3** have a crucial role in connecting three neighbouring complex units. Besides the water molecule, in the same structure, the N–H donors are atoms N1, N2 and N4 while the acceptors are all three oxygen atoms of nitrato coligand. (Fig. S-4 of the Supplementary material). Two neutral complexes are connected *via* N2–H2···O1 and N4–H4B···O2 hydrogen bonds (Table II) forming the centrosymmetric dimers, while water molecules interconnect these dimers

via O4–H4D···Cl1 hydrogen bonds forming the chain of dimers shown in Fig. S-5a of the Supplementary material, where one dimer present pair of the green and blue model. These chains of dimers are interconnected also by the same water molecules, through O4–H4C···O2 and by ligand and nitrato coligand through N2–H2···O3 hydrogen bond (Fig. S-5b). On the other hand, there is a network of the same interconnected chains which is centrosymmetric in relation to the previously described one where there is stacking of pyridine aromatic ring and metallocycle Cu1–N1–C1–N2–N3 (Fig. S-6 of the Supplementary material), but with no hydrogen bonding between those two (Fig. S-5c).

TABLE II. Geometrical parameters for hydrogen bonds

D–H···A	*d*(H···A) / Å	*d*(D···A) / Å	∠(D–H···A) / °	Symmetry operation for A
		1		
N1–H1···O3	2.11(2)	2.941(3)	175(3)	$-x+1, y+1/2, -z+3/2$
N2–H2···O2	2.06(2)	2.893(3)	172(2)	x, y, z
N4–H4A···O2	2.14(2)	2.973(3)	175(3)	$-x+1, y+1/2, -z+3/2$
N4–H4B···O1	2.06(2)	2.892(3)	176(3)	x, y, z
		2		
N4–H4B···N2	2.21(2)	3.057(2)	169(2)	$-x+1, -y+1, -z+2$
N4–H4A···Cl1	2.57(2)	3.3618(19)	166(2)	$-x+1, -y+2, -z+1$
		3		
O4–H4C···O2	2.28(2)	3.004(2)	158(3)	$x-1, y-1, z$
O4–H4D···Cl1	2.49(2)	3.3017(18)	170(3)	$-x+1, -y, -z$
N4–H4A···O4	2.04	2.826(2)	152.2	x, y, z
N4–H4B···O2	2.08	2.934(2)	171.9	$-x+1, -y+1, -z$
N1–H1···O4	2.49	3.1408(19)	133.2	x, y, z
N2–H2···O3	2.57	3.0933(19)	120.1	$x-1, y, z$
N2–H2···O1	2.10	2.8750(16)	149.3	$-x+1, -y+1, -z$

*Thermal properties of complexes **1**–**3***

All three compounds were analysed by simultaneous TG-DTG and online coupled TG–MS measurements in argon. Complex **1** begins to lose mass somewhat above room temperature, which causes a broad low-intensity mass change of 0.9 % up to ~130 °C (Fig. 2). This mass loss is most probably the result of the lattice water evaporation. The measured mass loss is somewhat less than the water content calculated based on crystallographic data (1.3 %) due to the spontaneous evaporation at room temperature during storage. The spontaneous water loss is in accordance with the tight empty space which H_2O can occupy in the crystal structure of the monoperiodic cation of **1**. The thermal decomposition of anhydrous **1** begins at 215 °C, onset. A sharp mass loss step of 31.0 % is characteristic of the decomposition. Following, the nitrate can be marked as the most reactive component of complex **1**, and in this step, it most probably decomposes also causing the oxidative decomposition of the organic ligand. Due to such

redox processes, the crystal lattice very likely crushes, too at this step. Above ~230 °C the decomposition continues at a steady rate without any stable intermediate formation, and it is not finished up to 700 °C.

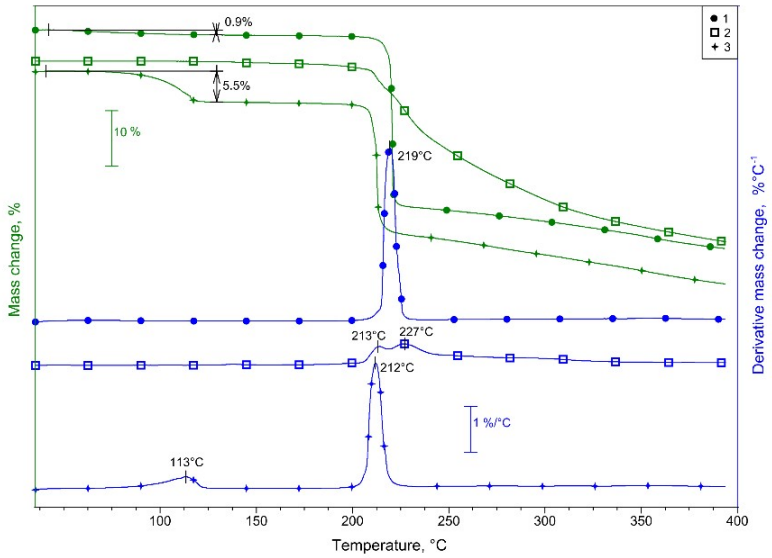

Fig. 2. TG and DTG curves of complexes **1**–**3** in argon.

Complex [Cu(L–H)Cl] (**2**) is stable up to 130 °C, onset. At this temperature, its mass is decreasing by 0.3 %. Considering that this complex does not contain lattice water, the mass loss in this step is most probably the result of the evaporation of water traces from the slightly hygroscopic compound. Above 190 °C complex **2** decomposes in several highly overlapped steps continuously without the formation of any stable intermediate. Its decomposition above 190 °C is not sharp as the decomposition of complexes **1** and **3**, because of the absence of nitrate and for the same reason its slighter decomposition process was expected, too.

The complex $[Cu(L)ClNO_3]\cdot H_2O$ (**3**) contains lattice water, which evaporates during the first mass loss step with DTG maximum at 113 °C. This was also proved by coupled TG–MS measurements. The measured mass loss of 5.5 % is a little bit higher than the mass percent of lattice water (5.06 %). Since compound **2** shows a slight hygroscopicity, the difference between the measured and calculated water content may originate from the absorbed humidity in this case too. The anhydrous **3** is stable up to 204 °C, onset. Above this temperature, the decomposition begins with a sharp mass loss step with the DTG maximum at 212 °C. The intensive mass loss is the result of the rapid decomposition of nitrate from **3**, like in the case of complex **1**. Above 219 °C the decomposition continues

at a steady rate without the formation of any stable intermediate, and it is not finished up to 700 °C.

The DSC data of the compounds are in accordance with their composition. The evaporation processes are endothermic, while the decomposition of the complexes is in all three cases exothermic. The exothermic effect of the thermal degradation of **1** and **3** was expected because of the presence of the nitrate group. Differently, in the case of **2**, the exothermicity of the decomposition process was not in prospect because it does not contain oxidative groups. However, due to the presence of nitrate, the exothermic effect, which follows the decomposition of complexes **1** and **3** is more intensive than that of complex **2** (Fig. 3) without nitrates. There is a difference between the intensity of the exothermic effect of **1** and **3**, also. The highest exothermic effect follows the decomposition of **1** with a polymeric structure. Despite that **1** is stable at somewhat higher temperatures than **3**, when it decomposes, more energy is released than from complex **3**, which leads to a higher exothermic effect in the case of **1**.

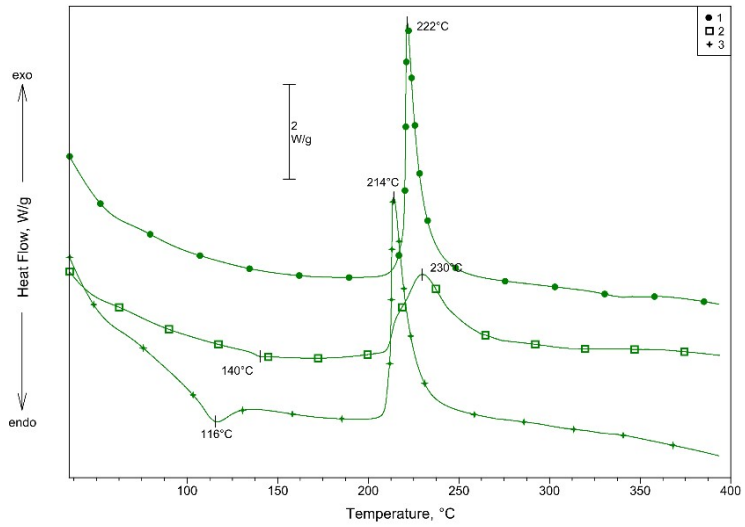

Fig. 3. DSC curves of complexes **1**–**3** in argon.

The TG–MS data prove the conclusions based on TG and DSC curves (Figs. 2 and 3). The first mass loss below 150 °C is in all three compound water evaporation. Even though compound **2** is synthesised in the absence of water and in the presence of NH_3, the following TG–MS signals suggest the presence of water (18 and 17 *m*/*z*) and not ammonia (17 and 16 *m*/*z*, Fig. 4). To follow the main decomposition step of the compounds, besides water (OH^+, H_2O^+), ammonia (NH_2^+, NH_3^+), and chlorine fragments (Cl^+, HCl^+) the signals of the nitrate decompo-

sition products NO^+, N_2O^+ and NO_2^+ were also analysed. From these fragments, the most intensive is NO^+ (30 *m*/*z*), which is usual for nitrate decomposition (Fig. 5).[24] The very small peak of 30 *m*/*z* in complex **2** cannot be correlated to NO^+ release because of the absence of nitrate. However, the mass value of 30 *m*/*z* may be correlated to the fragment N_2H_2 from the nitrogen-rich ligand. As is shown in Fig. S-7 of the Supplementary material, all the detected signals of complex **2** are the most intensive at the beginning of the thermal decomposition process.

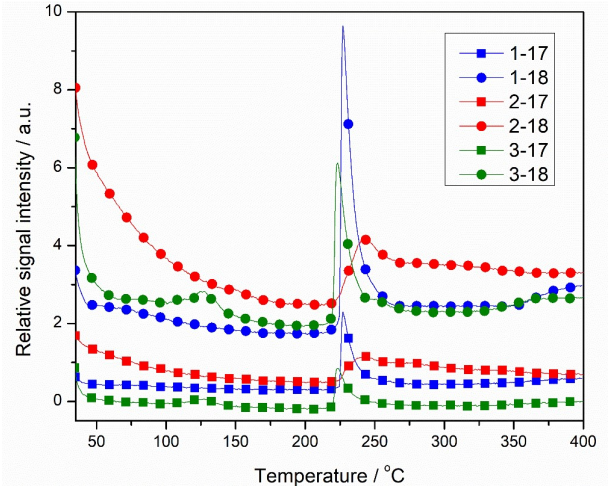

Fig. 4. MS curves of H_2O (17 and 18 *m*/*z*).

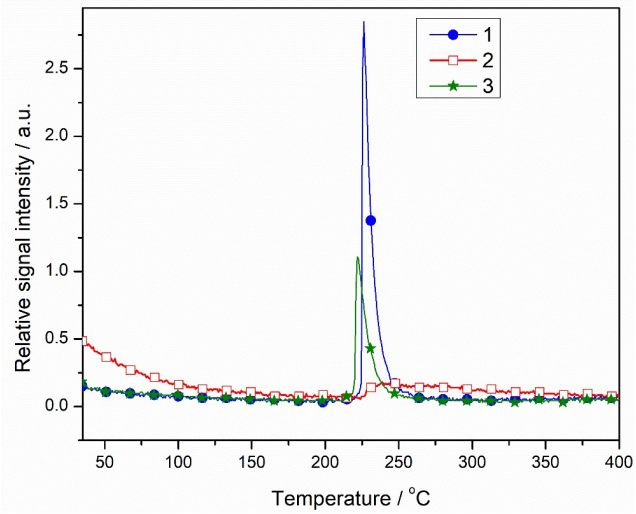

Fig. 5. MS curves of NO (30 *m*/*z*).

CONCLUSION

In the reaction of warm solutions of the ligand, $[H_2L]Cl_2$ and copper(II) nitrate, in the presence of different deprotonating agents, single-crystals of three new coordination compounds were formed – polymeric complex $\{[Cu(L)(\mu\text{-}Cl)]NO_3 \cdot H_2O\}_n$ (**1**) and neutral complexes [Cu(L–H)Cl] (**2**) and $[Cu(L)ClNO_3] \cdot H_2O$ (**3**), where L is 2-acetylpyridine-aminoguanidine. The ligand was coordinated in its neutral form in complexes **1** and **3**, where pyridine and lithium-acetate were used for deprotonation. As a stronger base, ammonia as deprotonating agent, in complex **2**, causes the coordination of the monoanion of the ligand. The Schiff base is coordinated through pyridine, azomethine, and the imine nitrogen atom. This coordination mode results in the formation of two five--membered chelate rings. Copper (II) is situated in the square-pyramidal environment of donor atoms of the ligand and its co-ligands in **1** and **3**, while copper (II) in **2** is placed in a square-planar environment of N-donor atoms and one chlorido ligand. The thermal measurements proved that complexes **1** and **2** are hygroscopic and by increasing the temperature lose the bonded water. Complex **3** also loses its lattice water during heating. All compounds are stable in their anhydrous form up to 200 °C and above this temperature they decompose. The beginning of their decomposition process is more intensive in **1** and **3** because of the presence of nitrate.

Different coordination behaviour of the ligand, in the presence of diprotonation agents with different base constants, can lead to different properties of these novel complexes, and further research will include the investigation of photoluminescence and the antioxidant properties will be analysed.

SUPPLEMENTARY MATERIAL

Additional data and information are available electronically at the pages of journal website: https://www.shd-pub.org.rs/index.php/JSCS/article/view/12476, or from the corresponding author on request. CCDC 2269543-2269546.CCDC 2279826–2279828 contain the supplementary crystallographic data for this paper. These data can be obtained free of charge from The Cambridge Crystallographic Data Centre (https://www.ccdc.cam.ac.uk/structures).

Acknowledgements. The authors gratefully acknowledge the financial support of the Ministry of Science, Technological Development and Innovation of the Republic of Serbia (Grant No. 451-03-47/2023-01/200125), as well as Slovenian–Serbian joint co-operation project funded by Ministry of Science, Technological Development and Innovation of the Republic of Serbia and Slovenian Research and Innovation Agency (2023–2025).

ИЗВОД

РЕАКЦИЈЕ 2-АЦЕТИЛПИРИДИН-АМИНОГВАНИДИНА СА Cu(II) ПОД РАЗЛИЧИТИМ РЕАКЦИОНИМ УСЛОВИМА

МАРИЈАНА С. КОСТИЋ, НИКОЛА Д. РАДНОВИЋ, МАРКО В. РОДИЋ, БЕРТА БАРТА ХОЛО, ЉИЉАНА С. ВОЈИНОВИЋ ЈЕШИЋ и МИРЈАНА М. РАДАНОВИЋ

Универзитет у Новом Саду, Природно–математички факултет, Трг Доситеја Обрадовића 3, 21000 Нови Сад

Деривати аминогванидина су већ дуже време у фокусу истраживања захваљујући разноврсној биолошкој активности као што су антивирусна, антибактеријска, аналгетска, антиоксидативна, као и антиканцерогена активност. Њихови комплекси са металима су такође испитивани и поред биолошки активних деривата аминогванидина велики број ових комплекса такође показује значајну биолошку активност. Осим тога, неки показују значајна фотолуминесцентна својства и користе се за фотоелектронске уређаје. У складу са свим наведеним, у овом раду су приказане синтезе, физичко–хемијска, структурна и термоаналитичка карактеризација комплекса 2-ацетилпиридин аминогванидина (L) са бакром(II). При различитим реакционим условима Cu(II) са L даје комплексе различитог састава. Показано је да се наведена Шифова база може координовати у неутралној или моноанјонској форми у зависности од јачине базе коришћене за депротонацију. У присуству пиридина је добијен координациони полимер, док у присуству амонијака/литијум-ацетата добијена су два различита мономерна комплекса. Одређена су њихова физичко–хемијска и термичка својства, као и молекулска и кристална структура.

(Примљено 7. јула, ревидирано 28. јула, прихваћено 8. септембра 2023)

REFERENCES

1. O. Dömötör, N. V. May, G. T. Gál, G. Spengler, A. Dobrova, V. B. Arion, É. A. Enyedy, *Molecules* **27** (2022) 2044 (https://doi.org/10.3390/MOLECULES27072044/S1)
2. J. Vojtaššák, J. Čársky, L. Danišovič, D. Böhmer, M. Blaško, T. Braxatorisová, *Toxicol. in Vitro* **20** (2006) 868 (https://doi.org/10.1016/j.tiv.2005.12.009)
3. C. Watala, M. Dobaczewski, P. Kazmierczak, J. Gebicki, M. Nocun, I. Zitnanova, O. Ulicna, Z. Durackova, I. Waczulíková, J. Carsky, S. Chlopicki, *Vascul. Pharmacol.* **51** (2009) 275 (https://doi.org/10.1016/j.vph.2009.07.002)
4. Yu. M. Chumakov, V. I. Tsapkov, G. Bocelli, B. Ya. Antosyak, S. G. Shova, A. P. Gulea, *Crystallogr. Rep.* **51** (2006) 60 (https://doi.org/10.1134/S1063774506010123)
5. M. S. More, P. G. Joshi, Y. K. Mishra, P. K. Khanna, *Mater. Today Chem.* **14** (2019) 100195 (https://doi.org/10.1016/j.mtchem.2019.100195)
6. C. Boulechfar, H. Ferkous, A. Delimi, A. Djedouani, A. Kahlouche, A. Boublia, A. S. Darwish, T. Lemaoui, R. Verma, Y. Benguerba, *Inorg. Chem. Commun.* **150** (2023) 110451 (https://doi.org/10.1016/j.inoche.2023.110451)
7. S. S. Chourasiya, D. Kathuria, S. S. Nikam, A. Ramakrishnan, S. Khullar, S. K. Mandal, A. K. Chakraborti, P. V. Bharatam, *J. Org. Chem.* **81** (2016) 7574 (https://doi.org/10.1021/acs.joc.6b01258)
8. M. G. Jelić, D. G. Georgiadou, M. M. Radanović, N. Ž. Romčević, K. P. Giannakopoulos, V. M. Leovac, L. F. Nađ, L. S. Vojinović-Ješić, *Opt. Quantum Electron.* **48** (2016) 276 (https://doi.org/10.1007/s11082-016-0547-5)
9. V. M. Leovac, M. D. Joksović, V. Divjaković, L. S. Jovanović, Ž. Šaranović, A. Pevec, *J. Inorg. Biochem.* **101** (2007) 1094 (https://doi.org/10.1016/j.jinorgbio.2007.04.004)

10. L. S. Vojinović-Ješić, M. M. Radanović, M. V. Rodić, V. Živković-Radovanović, L. S. Jovanović, V. M. Leovac, *Polyhedron* **117** (2016) 526 (https://doi.org/10.1016/J.POLY.2016.06.032)
11. M. M. Radanović, M. V. Rodić, L. S. Vojinović-Ješić, S. Armaković, S. J. Armaković, V. M. Leovac, *Inorg. Chim. Acta* **473** (2018) 160 (https://doi.org/10.1016/J.ICA.2017.12.038)
12. M. Radanovic, S. Novakovic, M. Rodic, L. Vojinovic-Jesic, C. Janiak, V. Leovac, *J. Serb. Chem. Soc.* **87** (2022) 1259 (https://doi.org/10.2298/JSC220613072R)
13. M. M. Radanović, L. S. Vojinović-Ješić, M. G. Jelić, E. Sakellis, B. Barta Holló, V. M. Leovac, M. V. Rodić, *Inorganics (Basel)* **10** (2022) 147 (https://doi.org/10.3390/inorganics10100147)
14. M. M. Radanović, M. V. Rodić, L. S. Vojinović-Ješić, S. Armaković, S. J. Armaković, V. M. Leovac, *Inorg. Chim. Acta* **473** (2018) 160 (https://doi.org/10.1016/j.ica.2017.12.038)
15. G. M. Sheldrick, *Acta Crystallogr. A Found. Adv.* **71** (2015) 3 (https://doi.org/10.1107/S2053273314026370)
16. G. M. Sheldrick, *Acta Crystallogr., C* **71** (2015) 3 (https://doi.org/10.1107/S2053229614024218)
17. A. L. Spek, *Acta Crystallogr., D* **65** (2009) 148 (https://doi.org/10.1107/S090744490804362X)
18. C. R. Groom, I. J. Bruno, M. P. Lightfoot, S. C. Ward, *Acta Crystallogr., B* **72** (2016) 171 (https://doi.org/10.1107/S2052520616003954)
19. I. J. Bruno, J. C. Cole, M. Kessler, J. Luo, W. D. S. Momerwell, L. H. Purkis, B. R. Smith, R. Taylor, R. I. Cooper, S. E. Harris, A. G. Orpen, *J. Chem. Inf. Comput. Sci.* **44** (2004) 2133 (https://doi.org/10.1021/CI049780B)
20. C. F. MacRae, I. Sovago, S. J. Cottrell, P. T. A. Galek, P. McCabe, E. Pidcock, M. Platings, G. P. Shields, J. S. Stevens, M. Towler, P. A. Wood, *Urn:Issn:1600-5767* **53** (2020) 226 (https://doi.org/10.1107/S1600576719014092)
21. K. Nakamoto, *Infrared and Raman spectra of inorganic and coordination compounds. Part B, Applications in coordination, organometallic, and bioinorganic chemistry*, Wiley, New York, 2009 (ISBN 978-0-471-74339-2)
22. A. W. Addison, T. N. Rao, J. Reedijk, J. van Rijn, G. C. Verschoor, *J. Chem. Soc., Dalton Trans.* **0** (1984) 1349 (https://doi.org/10.1039/DT9840001349)
23. L. Yang, D. R. Powell, R. P. Houser, *J. Chem. Soc., Dalton Trans.* (2007) 955 (https://doi.org/10.1039/b617136b)
24. NIST Chemistry WebBook, https://webbook.nist.gov/chemistry/ (accessed June 30, 2023).